

Document downloaded from:

[\[http://redivia.gva.es/handle/20.500.11939/5732\]](http://redivia.gva.es/handle/20.500.11939/5732)

This paper must be cited as

[Munera S, Besada C, Blasco J, Cubero S, Salvador A, Talens P, Aleixos N (2017). Astringency assessment of persimmon by hyperspectral imaging. *Postharvest Biology and Technology*, 125, 35-41.]

ivia
Institut Valencià
d'Investigacions Agràries

The final publication is available at

[\[http://dx.doi.org/10.1016/j.postharvbio.2016.11.006\]](http://dx.doi.org/10.1016/j.postharvbio.2016.11.006)

Copyright [Elsevier]

1 **Astringency assessment of persimmon by hyperspectral imaging**

2 **Sandra Munera^{1(*)}, Cristina Besada^{2(*)}, José Blasco¹, Sergio Cubero¹, Alejandra Salvador², Pau Talens³,**
3 **Nuria Aleixos^{4(**)}**

4

5 ¹⁾Centro de Agroingeniería. Instituto Valenciano de Investigaciones Agrarias (IVIA). Ctra. Moncada-Náquera
6 Km 4.5, 46113, Moncada, Valencia (Spain)

7 ²⁾Centro de Tecnología Postcosecha. Instituto Valenciano de Investigaciones Agrarias (IVIA). Ctra. Moncada-
8 Náquera Km 4.5, 46113, Moncada, Valencia (Spain)

9 ³⁾Departamento de Tecnología de Alimentos. Universitat Politècnica de València. Camino de Vera, s/n, 46022
10 Valencia (Spain)

11 ⁴⁾Departamento de Ingeniería Gráfica. Universitat Politècnica de València. Camino de Vera, s/n, 46022
12 Valencia (Spain)

13

14 * These authors contributed equally

15 **E-mail of the corresponding author: naleixos@dig.upv.es

16

17 **ABSTRACT**

18 One of the current challenges of persimmon postharvest research is the development of
19 non-destructive methods that allow determination of the internal properties of the fruit,
20 such as maturity, flesh firmness and astringency. This study evaluates the usefulness of
21 hyperspectral imaging in the 460–1020 nm range as a non-destructive tool to achieve these
22 aims in Persimmon cv. ‘Rojo Brillante’ which is an astringent cultivar. Fruit were harvested
23 at three different stages of commercial maturity and exposed to different treatments of CO₂
24 (95% CO₂ – 20 °C – from 0 to 24 h) in order to obtain fruit with different levels of
25 astringency. Partial Least Square (PLS) based methods were used to classify persimmon
26 fruits by maturity and to predict flesh firmness from the average spectrum of each fruit. The
27 results showed a 97.9% rate of correct maturity classification and an R²_P of 0.80 for
28 firmness prediction with only five selected wavelengths. For astringency assessment, as our
29 results showed that the soluble tannins that remain after CO₂ treatments are distributed
30 irregularly inside the flesh, a model based on PLS was built using the spectrum of every
31 pixel in the fruit. The model obtained an R²_P of 0.91 which allowed the creation of the
32 predicted distribution maps of the tannins in the flesh of the fruit, thereby pointing to
33 hyperspectral systems as a promising technology to assess the effectiveness of the

34 deastringency treatments that are usually applied before commercialising persimmons from
35 astringent cultivars.

36

37 *Keywords:* *Diospyros kaki*, fruit internal quality, soluble tannins, distribution map,
38 hyperspectral imaging, computer vision

39

40 **1. INTRODUCTION**

41 Astringency removal is required prior to commercialising astringent persimmon
42 cultivars. The astringency of persimmon fruit is due to the high soluble tannin content in
43 the flesh. Traditionally, the astringent cultivars have been consumed after fruit has been
44 submitted to an over-ripening treatment with exogenous ethylene; under these conditions
45 astringency removal is accompanied by a drastic loss of flesh firmness which hampers
46 postharvest handling of the fruit. For this reason, postharvest treatments which allow
47 astringency removal while preserving high flesh firmness have been developed in recent
48 years. Among them, the most widely used technique in commercial settings is based on
49 exposing fruits to high CO₂ concentrations (95% – 98%) for 24 h to 36 h. This method
50 promotes anaerobic respiration in the fruit, giving rise to an accumulation of acetaldehyde,
51 which reacts with the soluble tannins (ST). Tannins become insoluble at the end of the
52 treatment and astringency is no longer detected (Matsuo & Ito, 1982; Matsuo *et al.*, 1991).

53 The optimum duration of the CO₂ treatment depends on the cultivar but also on the stage
54 of fruit maturity (Besada *et al.*, 2010). If the treatment is too short, it may result in fruit
55 with residual astringency, and if extended excessively it may lead to losses of fruit quality
56 (Novillo *et al.*, 2014). Therefore, the optimum treatment conditions must be determined for
57 the different cultivars, but the stage of fruit maturity must also be taken into account.
58 Therefore, the knowledge of the fruit condition at harvest according to its stages of maturity
59 is a prerequisite to apply the adequate CO₂ treatment.

60 After application of the CO₂ treatment it is necessary to evaluate its effectiveness to
61 avoid residual astringency that could negatively affect the future buying intentions of
62 consumers. Currently, the effectiveness of deastringency treatment can be assessed by
63 measuring the content of ST that remain in the flesh, although this is a slow and destructive
64 analytical method, and thus commercially unfeasible. Another method to determine the

65 level of astringency of persimmon fruit is based on the reaction of ST (responsible for
66 astringency) with FeCl_3 , which leads to a blue staining; the intensity of the staining
67 observed after a slice of the flesh is impregnated with FeCl_3 depends on its level of ST.
68 Although this method is faster and easier than the analytical determination of ST, it is also
69 destructive and subjective and therefore it is necessary to search for new rapid, reliable,
70 non-contact and non-destructive techniques.

71 Among them, computer vision represents a fast, accurate, and proved alternative for
72 monitoring fruit quality (Cubero *et al.*, 2011). However, this kind of sensors are limited to
73 analysing the external properties of the fruit like colour, size or the presence of external
74 defects, not being capable of detecting internal compounds like ST, responsible of the
75 astringency. Therefore, other methods capable of analyse internal compounds are
76 necessary. Spectroscopy is a non-destructive, inexpensive, rapid and reliable technique that
77 has traditionally been used in food chemistry for qualitative and quantitative determination
78 of different compounds in fruit samples, especially near infrared (NIR) spectroscopy
79 (Nicolai *et al.*, 2007; Nicolai *et al.*, 2014; Magwaza *et al.*, 2012; López *et al.*, 2013). This
80 technique has been utilised for the quantitative determination of soluble solids content
81 (SSC), firmness, acidity, dry matter, chemical substances such as glucose, sucrose, citric
82 acid, malic acid, starch or cellulose in different fruits (Schmilovitch *et al.*, 2000; Nagle *et al.*,
83 *et al.*, 2010; Theanjumpol *et al.*, 2013), and even to determine a maturity index (Jha *et al.*,
84 2013), internal quality index (Cortés *et al.*, 2016) or different appropriate indices for quality
85 analysis (Attila and János, 2011).

86 However, a major disadvantage of spectroscopy is that only can measure in a single point
87 of the sample. On the other hand, hyperspectral imaging is a non-destructive optical
88 technology that integrates the advantages of spectroscopy and conventional imaging to
89 obtain both spatial and spectral information simultaneously. It allows the visualisation of
90 internal compounds of the fruit distributed into the image which is not possible with
91 conventional spectroscopy (Gowen *et al.*, 2007; Lorente *et al.*, 2012) as in the case of the
92 ST of the persimmon, leading to a non-valid probe measurement and forcing to take
93 measurements in many places of the fruit surface (Noypitak *et al.*, 2015). Thus, using
94 hyperspectral imaging Mendoza *et al.*, (2011) developed a method for the in-line prediction
95 of firmness and SSC achieving coefficient of correlation between 0.83 and 0.95 for

96 prediction of firmness and between 0.67 and 0.87 for prediction of SSC in different apple
97 cultivars. Later they compared several spectral sensors to predict these properties (Mendoza
98 *et al.*, 2012). Cen *et al.* (2016) investigated the detection of internal chilling injuries in
99 pickling cucumbers using hyperspectral reflectance (500–675 nm) and transmittance (675–
100 1000 nm) achieving 100% of correct detection using SVM with the fruit travelling at 100
101 mm/s, which gives an idea of the potential of this technology for non-destructive in-line
102 quality control.

103 Ripeness has been one of the main features studied with this technology. Lleó *et al.*
104 (2011) used hyperspectral imaging (400–1000 nm) to predict the maturity of ‘Rich lady’
105 peaches by computing different indices extracted from band ratios and combinations. The
106 application of these indices to create maps from the classification of individual pixels
107 showed that the ripening was not uniform throughout the entire fruit. Furthermore, the
108 ripening of intact bell peppers was studied by Schmilovitch *et al.* (2014) using
109 hyperspectral imaging (550–850 nm). They were able to relate some internal compounds
110 like SSC, total chlorophyll, carotenoid and ascorbic acid content with the spectral data by
111 means of a PLS regression, in all cases achieving an R^2 higher than 0.90 except for ascorbic
112 acid (0.72). The chemometric models they established were used to estimate internal
113 components in each pixel of the fruit image, thus allowing mapping of the quality
114 parameters in the intact peppers.

115 Apart from maturity, other properties can also be assessed. Yang *et al.* (2015) measured
116 anthocyanin content in lychee pericarp in the 350–1050 nm range. They created several
117 models achieving an R^2 of 0.92 using all wavelengths. The model was later applied to
118 entire fruits to create distribution maps with which to visualize the changes in anthocyanin
119 content during storage time. Liu *et al.* (2015) used multispectral images to predict lycopene
120 and phenolic compounds content in intact tomatoes. The comparison of methods based on
121 PLS, least squares-support vector machines (LS-SVM) and back propagation neural
122 networks (BPNN) showed BPNN to be the one that performed best, with an R^2 of 0.96. By
123 applying the model to each pixel of the tomato they were able to create prediction maps of
124 the intact tomatoes.

125 In persimmon fruit the use of this non-destructive technology to assess different quality
126 parameters is beginning to be studied. Hence, Wei *et al.* (2014) used hyperspectral imaging

127 to study the relationship between firmness and fruit maturity. Mohammadi *et al.* (2015)
128 also used image analysis techniques to evaluate the index of external colour of the fruits in
129 order to classify them into three stages of commercial maturity. Nevertheless, more studies
130 are necessary in this regard, particularly with fruit that will be commercialized with a firm
131 texture. Furthermore, to our knowledge, the potential of hyperspectral technology to detect
132 the level of astringency in persimmon has not been evaluated to date. Only some works
133 have been carried out to detect phenolic compounds related to astringency (Nogales-Bueno
134 *et al.*, 2014), focused especially on wine quality (Aleixandre-Tudó *et al.*, 2015; Boulet *et*
135 *al.*, 2016). And only one work has been found related to astringency in persimmon using
136 NIR spectroscopy in the range of 660-960 nm (Noypitak *et al.*, 2015).

137 The aim of this work is to advance in the development of a non-destructive tool to assess
138 the astringency of persimmon fruits that have been gone under deastringency treatment,
139 since at present there are no methods or previous research focused on this aim for this type
140 of fruit, being still a demand from the industry.

141

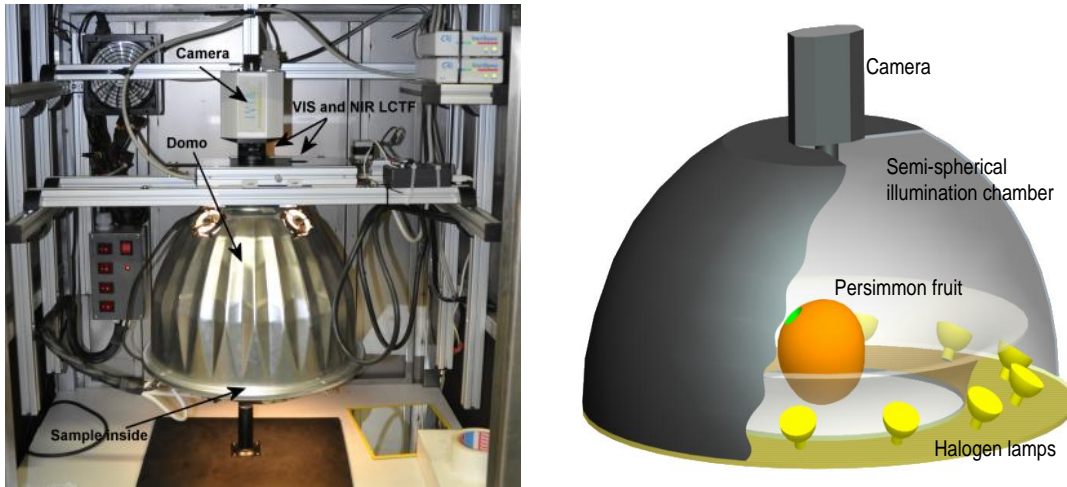
142 **2. MATERIALS AND METHODS**

143 **2.1. Image acquisition and calibration**

144 The hyperspectral imaging system capable of acquiring images in the spectral range
145 400–1100 nm was composed of an industrial camera (CoolSNAP ES, Photometrics, AZ,
146 USA), and two liquid crystal tunable filters (LCTF) (Varispec VIS-07 and NIR-07,
147 Cambridge Research & Instrumentation, Inc., MA, USA) and a lens capable of covering the
148 whole spectral range without losing the focus (Xenoplan 1.4/23, Schneider Optics,
149 Hauppauge, NY, USA). The system was configured to capture images of 1392 x 1040
150 pixels with a spatial resolution of 0.14 mm/pixel and a spectral resolution of 10 nm. To
151 optimise the dynamic range of the camera, prevent saturated images and correct the spectral
152 sensitivity of the different elements of the system, a calibration of the integration time of
153 each band was performed by capturing the averaged reflectance of a white reference target
154 (Spectralon 99%, Labsphere, Inc, NH, USA) corresponding to 90% of the dynamic range of
155 the camera. The scene was illuminated by 12 halogen spotlights of 37 W each (Eurostar IR
156 Halogen MR16. Ushio America, Inc., CA, USA) powered by direct current (12 V), which
157 lit the scene indirectly by means of diffuse reflection inside a hemispherical dome where

158 whole fruits were introduced manually (Fig. 1). The inner surface of the aluminium dome
 159 was painted in white and given a rough texture using a synthetic polish sprayer in order to
 160 reduce directional reflections that could cause bright spots, thus providing highly
 161 homogeneous light. A holder was used to place all samples at the same height inside the
 162 dome.

163



164 Figure 1. Configuration of the hyperspectral acquisition system

165

166 One hyperspectral image was captured of each fruit in reflectance mode in the working
 167 spectral range 460–1020 nm, which together formed a database with a total of 150
 168 hyperspectral images with 57 wavelengths each. Equation (1) (Gat, 2000) was used to
 169 obtain the corrected relative reflectance of a pixel in the position (x,y) of the
 170 monochromatic band λ .

171

$$172 \quad \rho_{xy}(x, y, \lambda) = \frac{R_{abs}}{R_{white}} = \rho^{Ref}(\lambda) \frac{R(x,y,\lambda) - R_{black}(x,y,\lambda)}{R_{white}(x,y,\lambda) - R_{black}(x,y,\lambda)} \quad (1)$$

173

174 where $\rho^{Ref}(\lambda)$ is the standard reflectance of the white reference target (99% in this work),
 175 $R(x,y,\lambda)$ is the reflectance of the fruit captured by the charge-coupled device (CCD) sensor
 176 of the camera, $R_{white}(x,y,\lambda)$ is the reflectance captured by the CCD of the white reference
 177 target, and $R_{black}(x,y,\lambda)$ is the reflectance captured by the CCD while avoiding any light
 178 source in order to quantify the electronic noise of the sensor.

179

180 **2.2. Plant material and experimental design**

181 Persimmon cv. 'Rojo Brillante' fruits were harvested in L'Alcudia (Valencia, Spain) at
182 three different stages of commercial maturity (M1, M2 and M3) corresponding to early and
183 late November, and mid-December. These three stages were intentionally selected in order
184 to obtain fruit with different degree of maturity and therefore of firmness, since the success
185 of the treatments depend on the fruit firmness at harvest (Salvador *et al.*, 2008) and
186 therefore the possibility of assessing the astringency in fruits with different firmness was
187 studied.

188 A total of 150 fruits with no skin damage and a homogeneous colour were selected and
189 individually evaluated, corresponding to 50 fruits for each stage of maturity. In order to
190 obtain different levels of astringency, fruits at each stage of maturity were divided into five
191 homogeneous lots of 10 fruits each. Then the fruit was exposed to CO₂ treatments in closed
192 containers (air containing 95% CO₂ at 20 °C and 90% RH) for 0 h, 6 h, 12 h, 18 h and 24 h.
193 Hyperspectral images of the intact fruits were acquired within 8 h after the CO₂ treatment.
194 In addition, the physicochemical parameters (external colour, firmness, ST and astringency)
195 to achieve the objectives of this study were evaluated individually in each fruit.

196

197 **2.3. Physicochemical analysis**

198 The external colour index ($CI=1000a/Lb$) was measured using a colorimeter (CR-300,
199 Konica Minolta Inc, Tokyo, Japan) to know the colour of the fruits in each maturity stage at
200 harvest. This index is based on the citrus colour index calculated using Hunter Lab colour
201 values (Jiménez-Cuesta *et al.*, 1981).

202 Flesh firmness was determined by means of a universal testing machine (4301, Instron
203 Engineering Corp., MA, USA) equipped with an 8 mm puncture probe. The crosshead
204 speed during testing was 1 mm/s. During the test, the force increased smoothly until it
205 decreased drastically when the flesh was broken, and then the maximum peak force was
206 registered. The results were expressed as the load (in N) required for breaking the flesh of
207 the fruit on both sides after peel removal.

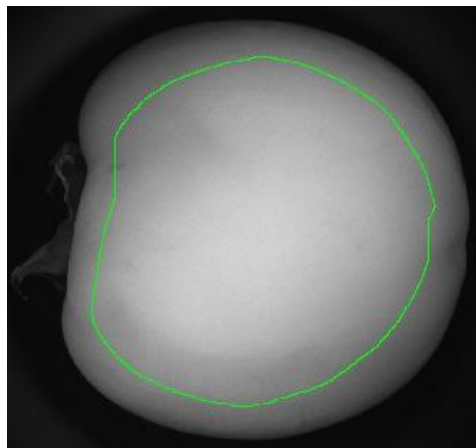
208 Analysis of variance (ANOVA) and Tukey's test were conducted to determine
209 significant differences during maturity (colour and firmness). For this purpose, the software
210 Statgraphics (Manugistics Corp., Rockville, Md.) was used.

211

212 **2.3.1 Assessment of firmness**

213 Among the physiological changes related to fruit maturation, such as colour or decline
214 of ST (Salvador *et al.*, 2007), the change in fruit firmness is one of the most important
215 feature to determine the optimum postharvest condition. In this regard, Salvador *et al.*
216 (2008) reported that fruit firmness can influence the effectiveness of the CO₂ treatment
217 because the loss of pulp structure associated to fruit softening may difficult the diffusion of
218 CO₂. To know if firmness could be predicted using the hyperspectral imaging system, a
219 representative ROI of the whole fruit surface was selected avoiding the stem and dark
220 borders (Fig. 2). The average spectrum of the pixels in the ROI was calculated and
221 considered as the fruit sample. Two thirds of the fruits in each maturity stage were used to
222 build the models and the remaining fruits were used as prediction set. A pre-processing
223 Standard Normal Variate (SNV) was applied to the spectra in order to remove scatter
224 effects from the original spectral data.

225



226

227 Figure 2. Hyperspectral image of a persimmon with the selected ROI (centred on 640 nm)

228

229 Hyperspectral systems are complex equipments that provide a huge amount of data. It is
230 therefore important to investigate whether the assessment of maturity can be performed
231 using a reduced number of selected wavelengths. The Successive Projections Algorithm
232 (SPA) has been proposed as a novel variable selection strategy for multivariate calibration
233 (Araújo *et al.*, 2001), and its purpose is to select wavelengths whose information content is
234 minimally redundant. The SPA is a forward selection method that builds an ordered chain

235 of k variables where each element is selected in order to present the least collinearity with
236 the previous ones. The collinearity between variables is assessed by the correlation between
237 the respective column vectors of the calibration matrix. As it is an iterative method, this
238 means that several subsets containing up to k variables can be formed. Finally, in order to
239 choose the most appropriate subset, Multiple Linear Regression models are built to
240 compare them in the terms of the RMSE. In order to select the most important bands, SPA
241 was applied using MATLAB R2015a (The MathWorks, Inc. MA, USA) on the calibration
242 set of fruits.

243 PLS-discriminant analysis (PLS-DA) was applied in order to know if it was possible to
244 separate the fruit into the three stages of maturity at harvest using both, the entire spectrum
245 and only the variables selected by the SPA. In a similar way, PLS regression (PLS-R) was
246 used to predict the firmness including the data provided by the universal testing machine
247 instead of the stages of maturity. A single 10-fold cross-validation was used to choose the
248 optimal number of LV and accuracy and predictive capability of the PLS-R models were
249 evaluated by RMSE and coefficient of determination R^2 . The software used in this study
250 was The Unscrambler X 10.1 (CAMO Software, Oslo, Norway).

251

252 **2.3.2 Assessment of Astringency**

253 The level of astringency of each individual fruit was determined in three different ways:

- 254 1) Each fruit was cut in half and pressed against 10x10 cm filter paper soaked in a 5%
255 FeCl_3 solution, obtaining a blue print whose quantity and intensity gave information
256 about the ST content and its distribution. This process is an alternative technique to
257 the Folin-Denis method used in industry to determine the level of astringency in
258 fruit batches, and it has only been used to show visually the internal distribution of
259 the ST and its intensity.
- 260 2) A flesh sample from each fruit was frozen at $-20\text{ }^\circ\text{C}$ and later the content of ST was
261 analysed using the Folin-Denis method (Taira, 1995). The results were expressed as
262 relative ST in fresh weight, being the quantitative reference used in our analyses.
- 263 3) The level of astringency of the fruit was evaluated by a sensory panel consisting of
264 10 semi-trained staff members of IVIA familiar with persimmon fruit and

265 astringency attribute. Astringency was determined using a 5-point scale from 1-
266 non-astringent or absence of astringency to 5-intensely astringent.

267

268 To assess the astringency using the hyperspectral imaging system a new approach
269 was used. As the current method used in the industry is based on the printing of the
270 content and distribution of ST, the imaging system was used also to create maps of the
271 distribution of the ST. Hence, the individual spectrum of each pixel in the image was
272 used to predict the astringency of that pixel, thus using the spectral but also the spatial
273 information provided by an image-based technology. A PLS model was built using 12
274 persimmons from the whole set of fruits. Six fruits (two of each maturity stage) were
275 selected from the non-treated fruit, and thus considering as very astringent and another
276 six (two of each maturity stage) from the batch that were treated for 24 h.

277 A total of 67456 pixels labelled as astringent or non-astringent were selected from
278 the aforementioned fruits. The spectra of these pixels were used to build the PLS model
279 that was internally validated by means of a 10-fold cross-validation. The model was
280 then projected to the rest of the fruit to obtain maps of the distribution of the
281 astringency in the fruits.

282

283 3. RESULTS AND DISCUSSION

284 3.1. Assessment of firmness

285 The colour index and the firmness of the samples at harvest are shown in Table 1. It is
286 observed that the firmness value decreases as the fruit ripen, but in all cases studied having
287 high firmness. In the case of the colour, the values measured indicate that fruit was
288 changing from orange to red, as the increasing of the CI is due to an increase of the *a* value
289 and a reduction of *b*, both variables expressed in Hunter Lab values.

290

291 Table 1. Colour index and firmness values for the three stages of maturity at harvest

	M1	M2	M3
CI	9.46 ± 1.77 ^a	18.20 ± 3.32 ^b	21.6 ± 4.05 ^c
Firmness (N)	43.85 ± 4.1 ^a	30.8 ± 3.5 ^b	24.4 ± 4.9 ^c

292 Values are mean \pm standard deviation. Different superscript letters in the same row indicate significant
 293 differences between groups (p -value <0.05), according to Tukey's test
 294

295 The SPA used to reduce the dimensionality achieved an optimal set of five wavelengths
 296 (570, 590, 680, 710, 990 nm). These wavelengths are associated to the range of absorption
 297 bands of carotenoids (570 and 590 nm) (Choudhary *et al.*, 2009; Merzlyak *et al.*, 2003),
 298 chlorophyll (680 and 710 nm) (Lleó *et al.*, 2011; Rajkumar *et al.*, 2012) and water content
 299 (990 nm) (Lu and Peng, 2006).

300 Table 2 shows the results obtained for the classification of persimmon fruits in terms of
 301 their stage of maturity. Both models, using all and the optimal wavelengths, achieved high
 302 percentage of fruits classified correctly ($>90\%$). As regarding the classification of each
 303 maturity stage, fruits of M2 were worst classified in both models.

304
 305 Table 2. Maturity classification (%) of the test set by PLS-DA using all and selected
 306 wavelengths

	#LV	Class	M1	M2	M3	Correct classification
All wavelengths	4	M1	94.6	0.9	0.0	93.9
		M2	4.0	91.5	4.4	
		M3	1.4	7.6	95.6	
Selected wavelengths	2	M1	92.9	2.7	0.0	90.0
		M2	4.9	86.3	9.1	
		M3	2.2	11.0	90.9	

307

308

309 Table 3 shows the results of the flesh firmness prediction, obtaining similar results using
 310 all and the selected wavelengths. Values obtained were 0.77 and 0.80 for R^2 of the
 311 prediction using all and selected wavelengths, respectively. The results were not as good as
 312 the prediction results of Wei *et al.* (2014), who achieved an R^2 value of 0.91, but they
 313 worked with non-treated fruit having higher firmness differences between the harvest and
 314 the marketing. In the case of 'Rojo Brillante' persimmon, if they are sold as firm fruit after
 315 receiving some treatment to remove astringency, values below 10 N are considered as
 316 unsuitable from a commercial point of view (Salvador *et al.*, 2004).

317

318 Table 3. Results of firmness prediction using PLS-R with all and selected wavelengths

	#LV	R^2_{CV}	RMSE _{CV}	R^2_P	RMSE _P
All wavelengths	2	0.80	4.34	0.77	3.89
Selected wavelengths	2	0.80	4.34	0.80	3.66

319

320 As stated, firmness is highly related to maturity, but also to astringency. As softening
 321 progresses further, acetaldehyde produced at rather low levels in the flesh also may
 322 promote tannin polymerization. Thus, in extremely soft fruit, both tannin-pectin complex
 323 formation and acetaldehyde-tannin polymerization may be involved in the reduction of
 324 astringency (Taira *et al.*, 1997). Then, it is very important for this fruit to demonstrate that
 325 deastringency treatments do not affect the firmness.

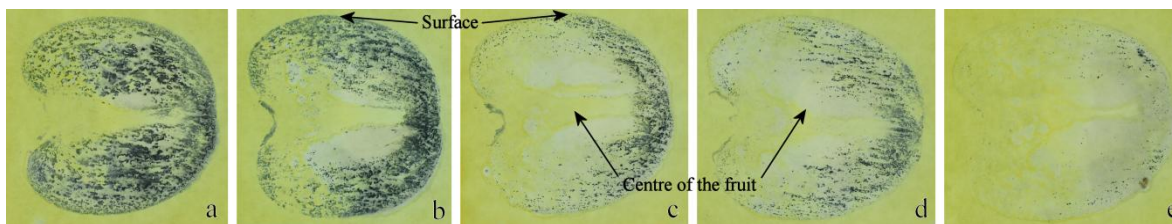
326

327 3.2. Astringency assessment

328 The application of the different CO₂ treatments resulted in fruit with a wide range of ST
 329 contents across the three stages of maturity studied, being the content of ST after different
 330 treatments between 0.75% and 0.03% (Fig. 3). This was supported by the sensory
 331 evaluation of the fruit (data not shown) that revealed that an ST content of 0.03% was
 332 related to non-astringent fruit, which is in agreement with Salvador *et al.*, (2007) and
 333 Besada *et al.*, (2010). ST contents higher than 0.4% led to intensely astringent fruit
 334 (sensory value of 5), while values between 0.04% and 0.4% were evaluated by the panellist
 335 as slight to medium astringency.

336 The evaluation of the ST by the FeCl₃ method revealed a progressive reduction of the ST
 337 in the fruit as the duration treatment was longer. Moreover, it was observed that the
 338 reduction of the ST advanced from the calyx area. Figure 3 shows examples of different
 339 blue prints obtained for the different duration of the CO₂ treatments.

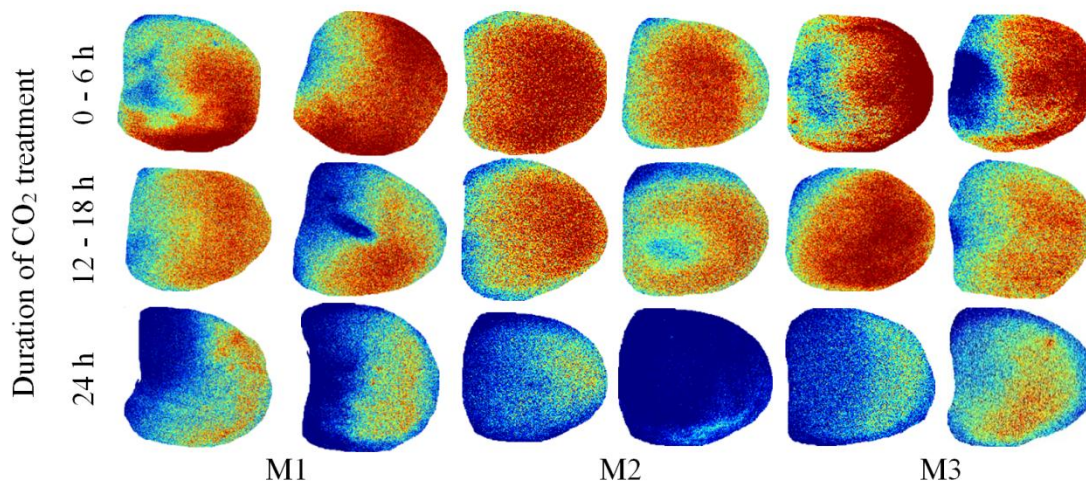
340



341

342 Figure 3. Astringency distribution from the blue print (FeCl_3) for persimmons CO_2 treated
343 during different hours: a) non-treated; b-e) treated with CO_2 for 6 h, 12 h, 18 h and 24 h
344

345 The model built from astringent and non-astringent pixels using PLS was used to predict
346 the astringency of the pixels of the validation fruits and to visually compare them with the
347 prints obtained using the destructive FeCl_3 method. Figure 4 shows several examples of the
348 predicted distribution map of the astringency of randomly chosen persimmons that were
349 treated with CO_2 for different periods to achieve different levels of astringency (from
350 untreated fruit that was evaluated by the panellist as intensely astringent to 24 h-treated
351 fruit, in which astringency was not detected, including medium or slight astringency for
352 fruit treated for 6 h, 12 h or 18 h). A colour scale was used, being non-astringent pixels
353 represented by the blue colour and astringents by red colour.
354



356

357 Figure 4. Samples of prediction maps from hyperspectral images of persimmons in the
 358 three maturity stages

359

360 Prediction maps obtained using hyperspectral imaging system showed astringency
 361 distribution on the surface of each fruit. It was observed that the distribution of astringency
 362 in fruits under different treatments followed a very similar pattern to one obtained using
 363 destructive methods based on FeCl_3 prints (Fig. 3). In Figure 4, it is clearly visible that
 364 fruits with no treatment (0 h) or very short (6 h) treatment had the highest astringency while
 365 models predicted lower astringency for fruits receiving treatment for 24 h. In addition, it
 366 was evident in all the images that most astringency concentrated at the bottom of the fruit,
 367 while began to be removed from the calyx area, following the same trend shown in Fig. 3.

368

369 This work contributes to lay the basis for future non-destructive tools capable to decide
 370 whether a persimmon is or not astringent in postharvest or contains residual astringency
 371 after a defective treatment, thus ensuring high quality fruit to consumers. Despite the
 372 penetration depth of the hyperspectral imaging that can be of few millimetres in the fruit,
 373 the blue prints showed that the tannins are distributed similarly in the internal part of the
 374 fruit and near the surface, and therefore can be captured by the hyperspectral images.
 375 Hence, hyperspectral imaging can be considered a valuable technique for the non-
 376 destructive evaluation of the astringency and a potential alternative to current destructive
 methods.

377 Results achieved coincide with those achieved by Noypitak *et al.* (2015). They carried
378 out a study for astringency by using spectrometry in the near-infrared zone (700–1050 nm)
379 and measured in twelve different parts of the fruit, later calculating the average of all the
380 measurements and obtaining results of around R^2 of 0.95. However, the authors worked
381 with very astringent persimmons and persimmons in which all astringency was completely
382 eliminated, avoiding the intermediate levels of astringency. Moreover, at a difference from
383 this study, the authors used plastic bags to remove the astringency of the fruits, thereby
384 causing a sharp loss of firmness that could have large influence the results.

385

386 **4. CONCLUSIONS**

387 The results of the present study showed VIS/NIR hyperspectral imaging to be a
388 promising non-destructive tool to assess the astringency of persimmon fruits that have been
389 gone under deastringency treatment. On one hand, the SPA method was used to select a
390 small set of wavelengths (570, 590, 680, 710, 990 nm) that allowed fruit classification
391 according to their stage of maturity using PLS-DA. The success rate obtained using the
392 entire spectrum was slightly higher than using only the five selected wavelengths, but in
393 both cases higher than 90%. In addition, an optimum prediction of the flesh firmness was
394 achieved using PLS regression. Moreover, using the selected wavelengths, the coefficient
395 of determination R^2_P was higher (0.80) than using the full spectrum (0.77).

396 On the other hand, it was built a predictive model that, applied to fruit submitted to
397 deastringency treatments, allowed to create maps of the distribution of the ST that were
398 compared visually with the traditional and subjective method based in the blue prints, to
399 differentiate non-astringent fruits from those completely or medium astringent, thus
400 creating a comprehensive non-destructive tool that can be used as alternative to the current
401 destructive method based on $FeCl_3$ prints. Therefore, hyperspectral imaging should be
402 considered as a potential non-destructive method to evaluate the effectiveness of the
403 deastringency treatments.

404

405 **ACKNOWLEDGEMENTS**

406 This work has been partially funded by the Instituto Nacional de Investigación y
407 Tecnología Agraria y Alimentaria de España (INIA) through projects RTA2012-00062-

408 C04-01, RTA2012-00062-C04-03 and RTA2013-00043-C02 with the support of FEDER
409 funds and by the Conselleria d' Educació, Investigació, Cultura i Esport, Generalitat
410 Valenciana, through the project AICO/2015/122. Sandra Munera thanks INIA for the grant
411 FPI-INIA #43 (CPR2014-0082) partially supported by FSE funds.

412

413 **REFERENCES**

414 Aleixandre-Tudó, J.L., Nieuwoudt, H. & Du Toit, W.J. (2015). Robust ultraviolet-visible
415 (UV-Vis) partial least squares (PLS) model for tannin quantification in red wine. *Journal*
416 *of Agricultural and Food Chemistry* 63, 1088–1098.

417 Araújo, M. C. U., Saldanha, T. C. B., Galvão, R. K. H., Yoneyama, T., Chame, H. C. &
418 Visani, V. (2001). The successive projections algorithm for variable selection in
419 spectroscopic multicomponent analysis. *Chemometrics and Intelligent Laboratory*
420 *Systems*, 57(2), 65–73.

421 Attila, N. & János, T. (2011). Sweet cherry fruit analysis with reflectance measurements.
422 *Journal Analele Universității din Oradea, Fascicula: Protecția Mediului*, 17, 263-270.

423 Besada, C., Salvador, A., Arnal, L. & Martínez-Jávega, J.M., (2010). Optimization of the
424 duration of deastringency treatment depending on persimmon maturity. *Acta*
425 *Horticulturae* 858, 69–74.

426 Boulet, J.C., Trarieux, C., Souquet, J.M., Ducasse, M.A., Caillé, S., Samson, A., Williams,
427 P., Doco, T. & Cheynier, V. (2016). Models based on ultraviolet spectroscopy,
428 polyphenols, oligosaccharides and polysaccharides for prediction of wine astringency.
429 *Food Chemistry* 190, 357–363.

430 Cen, H., Lu, R., Zhu, Q. & Mendoza, F. (2014). Nondestructive detection of chilling injury
431 in cucumber fruit using hyperspectral imaging with feature selection and supervised
432 classification. *Postharvest Biology and Technology* 111, 352–361.

433 Choudhary, R., Bowser, T. J., Weckler, P., Maness, N. O. & McGlynn, W. (2009). Rapid
434 estimation of lycopene concentration in watermelon and tomato puree by fiber optic
435 visible reflectance spectroscopy. *Postharvest Biology and Technology* 52, 103–109.

436 Cortés, V., Ortiz, C., Aleixos, N., Blasco, J., Cubero, S. & Talens, P. (2016). A new
437 internal quality index for mango and its prediction by external visible and near-infrared
438 reflection spectroscopy. *Postharvest Biology and Technology*, 118, 148-158.

439 Cozzolino, D., Kwiatkowski, M.J., Parker, M., Cynkar, W.U., Damberg, R.G., Gishen, M.
440 & Herderich, M.J. (2004). Prediction of phenolic compounds in red wine fermentations
441 by visible and near infrared spectroscopy. *Analytica Chimica Acta* 513, 73–80.

442 Cubero, S., Aleixos, N., Moltó, E., Gómez-Sanchis, J. & Blasco, J. (2011). Advances in
443 machine vision applications for automatic inspection and quality evaluation of fruits and
444 vegetables. *Food Bioprocess Technology* 4, 487–504.

445 *Food Chemistry* 173, 482–488

446 Gat, N. (2000). Imaging spectroscopy using tunable filters: A review. Technical report,
447 Opto-Knowledge Systems Inc. OKSI.

448 Gómez-Sanchis, J., Blasco, J., Soria-Olivas, E., Lorente, D., Escandell-Montero, P.,
449 Martínez-Martínez, J.M., Martínez-Sober, M. & Aleixos, N., (2013). Hyperspectral
450 LCTF-based system for classification of decay in mandarins caused by *Penicillium*
451 *digitatum* and *Penicillium italicum* using the most relevant bands and non-linear
452 classifiers. *Postharvest Biology and Technology* 82, 76-86.

453 Gowen, A. A., O'Donnell, C. P., Cullen, P. J., Downey, G., & Frias, J. M. 2007.
454 Hyperspectral imaging—an emerging process analytical tool for food quality and safety
455 control. *Trends in Food Science and Technology* 18, 590–598.

456 Jha, S.N., Jaiswal P, Narsaiah K, Sharma R, Bhardwaj R, Gupta M, Kumar R. (2013).
457 Authentication of mango varieties using near infrared spectroscopy. *Agricultural*
458 *Research*, 2(3):229 – 235. 3.

459 Jiménez-Cuesta MJ, Cuquerella J, Martínez-Jávega JM. (1981) Determination of a color
460 index for citrus fruit degreening. In *Proceedings of the International Society of*
461 *Citriculture*, Vol. 2, 750-753.

462 Liu, C., Liu, W., Chen, W., Yang, J. & Zheng, L. (2015). Feasibility in multispectral
463 imaging for predicting the content of bioactive compounds in intact tomato fruit. *Food*
464 *Chemistry* 173, 482-488.

465 Lleó, L., Roger, J.M., Herrero-Langreo, A., Diezma-Iglesias, B. & Barreiro, P. (2011).
466 Comparison of multispectral indexes extracted from hyperspectral images for the
467 assessment of fruit ripening. *Journal of Food Engineering* 104, 612–620.

468 Lopez, A., Arazuri, S., Garcia, I., Mangado, J., Jaren, C. (2013) A review of the application
469 of near-infrared spectroscopy for the analysis of potatoes. *J. Agric. Food Chem.*, 61,
470 5413–5424.

471 Lorente, D., Aleixos, N., Gómez-Sanchis, J., Cubero, S., García-Navarrete, O.L. & Blasco,
472 J., (2012). Recent advances and applications of hyperspectral imaging for fruit and
473 vegetable quality assessment. *Food Bioprocess Technology* 5, 1121–1142.

474 Lu, R. & Peng, Y., (2006). Hyperspectral Imaging for assessing peach fruit firmness.
475 *Biosystems Engineering* 93, 161–171.

476 Magwaza, L.S., Opara, U.L., Nieuwoudt, H., Cronje, P.J.R., Saeys, W. & Nicolaï, B.
477 (2012) NIR Spectroscopy Applications for Internal and External Quality Analysis of
478 Citrus Fruit-A Review. *Food and Bioprocess Technology* 5, 425-444

479 Matsuo, T. & Ito, S. (1982). A model experiment for de-astringency of persimmon fruit
480 with high carbon dioxide: in vitro gelation of kaki-tannin by reacting with acetaldehyde.
481 *Journal of Agricultural Food Chemistry* 46, 683–689.

482 Matsuo, T., Ito, S. & Ben-Arie, R. (1991). A model experiment for elucidating the
483 mechanism of astringency removal in persimmon fruit using respiration inhibitors.
484 *Journal of the Japanese Society for Horticultural Science* 60, 437–442.

485 Mendoza, F., Lu, R., Ariana, D., Cen, H. & Bailey B. (2011). Integrated spectral and image
486 analysis of hyperspectral scattering data for prediction of apple fruit firmness and
487 soluble solids content. *Postharvest Biology and Technology* 62, 149-160.

488 Mendoza, F., Lu, R. & Cen, H. (2012). Comparison and fusion of four nondestructive
489 sensors for predicting apple fruit firmness and soluble solids content. *Postharvest*
490 *Biology and Technology* 73, 89–98.

491 Merzlyak, M.N., Solovchenko, A.E. & Gitelson, A.A. (2003). Reflectance spectral features
492 and non-destructive estimation of chlorophyll, carotenoid and anthocyanin content in
493 apple fruit. *Postharvest Biology and Technology* 27, 197–211.

494 Mohammadi, V., Kheiralipour, K. & Ghasemi-Varnamkhasti, M. (2015). Detecting
495 maturity of persimmon fruit based on image processing technique. *Scientia Horticulturae*
496 184, 123–128.

497 Nagle, M., Mahayothee, B., Rungpichayapichet, P., Janjai, S. & Müller, J. (2010). Effect of
498 irrigation on near-infrared (NIR) based prediction of mango maturity. *Scientia*
499 *Horticulturae*, 125(4), 771-774.

500 Nicolai, B.M., Beullens, K., Bobelyn, E., Peirs, A., Saeys, W., Theron, K.I. & Lammertyn,
501 J. (2007). Non-destructive measurement of fruit and vegetable quality by means of NIR
502 spectroscopy: A review. *Postharvest Biology and Technology*, 46 (2), 99–118.

503 Nogales-Bueno, J., Hernández-Hierro, J.M. & Heredia, F.J. (2014). Determination of
504 technological maturity of grapes and total phenolic compounds of grape skins in red and
505 white cultivars during ripening by near infrared hyperspectral image: a preliminary
506 approach. *Food Chemistry* 152, 586–591.

507 Novillo, P., Salvador, A., Llorca, E., Hernando, I. & Besada, C. (2014). Effect of CO₂
508 deastringency treatment on flesh disorders induced by mechanical damage in
509 persimmon. *Biochemical and microstructural studies. Food Chemistry* 145, 453 – 463.

510 Noypitak, S., Terdwongworakul, A., Krisanapook, K. & Kasemsumran, S. (2015).
511 Evaluation of astringency and tannin content in ‘Xichu’ persimmons using near infrared
512 spectroscopy. *International Journal of Food Properties*, 18:1014–1028.

513 Salvador, A., Arnal, L., Besada, C., Larrea, V., Quiles, A. & Pérez-Munuera, I. (2007).
514 Physiological and structural changes during ripening and deastringency treatment of
515 persimmon cv. ‘Rojo Brillante’. *Postharvest Biology and Technology* 46, 181–188.

516 Salvador, A., Arnal, L., Besada, C., Larrea, V., Quiles, A. & Pérez-Munuera, I. (2008).
517 Reduced effectiveness of the treatment for removing astringency in persimmon fruit
518 when stored at 15 °C. *Physiological and microstructural study. Postharvest Biology and*
519 *Technology* 49, 340 – 347.

520 Salvador, A., Arnal, L., Carot, J.M., Carvalho, C.P. & Jabaloyes, J.M. (2006). Influence
521 of different factor son firmness and color evolution during the storage of persimmon cv.
522 ‘Rojo Brillante’. *Sensory and Nutritive Qualities of Food*, 71(2), 170–175.

523 Salvador, A., Arnal, L., Monterde, A. & Cuquerella, J. (2004). Reduction of chilling injury
524 symptoms in persimmon fruit cv 'Rojo brillante' by 1-MCP. *Postharvest Biology and*
525 *Technology* 33, 285–291.

526 Schmilovitch, Z., Ignat, T., Alchanatis, V., Gatker, J., Ostrovsky, V. & Felföldi, J. (2014).
527 Hyperspectral imaging of intact bell peppers. *Biosystems engineering Special Issue:*
528 *Image Analysis in Agriculture* 117, 83-93.

529 Schmilovitch, Z., Mizrach, A., Hoffman, A., Egozi, H. & Fuchs, Y. (2000). Determination
530 of mango physiological indices by near-infrared spectrometry. *Postharvest Biology and*
531 *Technology*, 19(3), 245-252.

532 Taira, S. (1995). Astringency in persimmon. In: Linskens, H.F., Jackson, J.F. *Fruit*
533 *Analysis*. Springer, Hannover, Germany, pp. 97–110.

534 Taira, S., Ono, M. & Matsumoto N. (1997) Reduction of persimmon astringency by
535 complex formation between pectin and tannins. *Postharvest Biology and Technology* 12,
536 265–271

537 Theanjumol, P., Self, G., Rittiron, R., Pankasemsu, T., & Sardud, V. (2013). Selecting
538 Variables for Near Infrared Spectroscopy (NIRS) Evaluation of Mango Fruit Quality.
539 *Journal of Agricultural Science*, 5(7).

540 Vélez-Rivera, N., Blasco, J., Chanona-Pérez, J., Calderón-Domínguez, G., Perea-Flores,
541 M.J., Arzate-Vázquez, I., Cubero, S. & Farrera-Rebollo, T. (2014). Computer vision
542 system applied to classification of “Manila” mangoes during ripening process. *Food and*
543 *Bioprocess Technology* 7, 1183-1194.

544 Wei, X., Liu, F., Qiu, Z., Shao, Y. & He, Y. (2014). Ripeness Classification of Astringent
545 Persimmon Using Hyperspectral Imaging Technique. *Food and Bioprocess Technology*
546 7, 1371–1380.

547 Yahaya, O.K.M., MatJafri, M.Z., Aziz, A.A. & Omar, A.F. (2015). Visible spectroscopy
548 calibration transfer model in determining pH of Sala mangoes. *Journal of*
549 *Instrumentation*, 10, T05002.

550 Yang, Y.C., Sun, D.-W. Pu, H., Wang, N.N. & Zhu, Z. (2015). Rapid detection of
551 anthocyanin content in lychee pericarp during storage using hyperspectral imaging
552 coupled with model fusion. *Postharvest Biology and Technology* 103, 55–65.

553